Master thesis submitted to the College of Science and Engineering in partial fulfilment of the requirements for the degree of Master of Engineering Science (Biomedical) at Flinders University, Adelaide, South Australia

A SYSTEM TO ANALYSE PARA-ATHLETE MOVEMENT OUTSIDE THE LABORATORY

Research by:

Shweta Saha

Supervisors: Prof. Mark Taylor, Prof. David Hobbs, and Ms Lauren Wearne

Advisor: Dr David Haydon

Disclaimer

I certify that this thesis does not incorporate without acknowledgement any material previously submitted for a degree or diploma in any university and that to the best of my knowledge and belief, it does not contain any material previously published or written by another person in accordance with the University's policy on plagiarism. Unless otherwise referenced, all material presented in this report is my own.

Shweta Saha

December 2021

Acknowledgement

This work is supported by the College of Science and Engineering, Flinders University, Tonsley, South Australia. I would like to thank my supervisors under the guidance and inspiration I have done my Project Report, Prof. Mark Taylor, Prof. David Hobbs, and Ms Lauren Wearne. Also, I would like to thank South Australian Sports Institute (SASI) and Dr David Haydon for giving me the opportunity to work for them. I would like to acknowledge the knowledge received from Mr Robert Trott and Mr Michael Russo and the help received from Mr Craig Dorson and Miss Fiona Cramer. Furthermore, I would like to thank A./Prof Dominic Thewlis from the University of Adelaide for his support with his markerless motion capture system. I would also like to acknowledge Mr Christopher Kurrin Whalley for helping me post-processing the video obtained from the ZED2i camera. They have encouraged me with their motivational comments and trust during this process. I would like to thank the College of Science and Engineering, Flinders University, Tonsley, for supporting all the necessary equipment, technical support, and documents required to complete the Project Report.

Abstract

Sometimes winning or losing an athletic event comes down to the last second, so analysing the time taken to complete an entire phase cycle can help enhance an athlete's performance. Similarly, in Paralympic rowing, phase cycle analysis is essential to improve a para rowers performance.

Several studies have been conducted to analyse the kinematics of a para-rower, but all studies have been done on an ergometer. Currently, the most standardised motion capture system is the VICON system, but it requires an indoor set-up, making it a static system. Thus, the environmental factors like the resistance provided by the water and wind, which can influence the performance of a para-rower, have been neglected.

Therefore, this study aims to develop a device that can be used outdoors, like water. The rowing data in a Legs, Trunk, and Arms (LTA) set-up, was collected using the VICON motion camera system and the markerless ZED2i motion camera system. The data was collected for the joint angles, i.e., elbow, shoulder and hip. The data was processed using the VICON NEXUS 2.12.1 for the VICON motion camera system. The data for the markerless ZED2i motion camera system was processed using the OpenPose system, developed by A./Prof Dominic Thewlis.

The data obtained from the ZED2i OpenPose system was analysed against the VICON NEXUS 2.12.1 data set for a phase of an entire rowing cycle. From analysing data from the devices, it can be concluded that the ZED2i OpenPose markerless motion capture system can be used as a standalone markerless motion capture system.

Table of Contents

Table of Figures

Chapter 1: Introduction

Rowing is a recreational and competitive water activity growing worldwide the world. Pararowing was introduced to the Paralympic programme in Beijing in 2008. When participating in Paralympic sport, individuals with mobility and cognitive impairment have experienced improved health and wellness and increased levels of community integration, quality of life, psychological well-being and life satisfaction (Cutler, et al., 2016).

In rowing, a vital role is being played by the trunk, arms and lower body to accelerate and balance the boat. This study focuses on para-athlete rowers as, unlike the able-bodied rower, para-athlete rowers are unable to use all their body parts whilst rowing. Based on the level of ability, para-rowing has been classified into three categories. These categories are PR1, para-rowers with functional shoulders and arms (SA); PR2 are para- rowers who have functional Trunk and Arms (TA); and PR3 are para- rowers who have functional Legs, Trunk, and Arms (LTA). In PR3, impairments could include a loss of leg muscle control or impairments to 3 or more fingers. Each of these categories requires specific seating and strapping configurations based on their requirement and as per the rules of para-rowing (Severin, et al., 2021).

Earlier studies have been conducted to understand the kinematics of para rowers, but all studies have been conducted in an indoor environment on an ergometer. The most standardised motion capture system is the VICON motion capture system. Still, it has certain limitations, namely an indoor set-up, which restricts the rower to a stationary ergometer. Also, it requires marker placements for developing a stick figure of the participant. Therefore, vital factors like wind and water fluid dynamics, which play an essential role in rowing, are neglected. How a paraathlete rower overcomes, these environmental factors with their limitations are overlooked. So this study aims to develop a motion capture device that can be undertaken outdoors on the water. Thus, the developed motion capture device needs to be small, compact, lightweight, portable, and waterproof. Furthermore, this markerless motion capture system was validated against the gold standard VICON system.

Figure removed due to copyright restriction

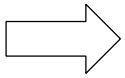

Figure 1: Aim of the study to take motion capture system outdoor to capture kinematic of the para-athlete rower

To achieve this goal, three complete stroke cycles of rowing will be analysed of the markerless motion capture system, ZED2i OpenPose system, against the standard VICON motion capture system. Figure 2 depicts an entire stroke of a rowing cycle, and the goal of this study is to analyse three such stroke cycles.

Figure removed due to copyright restriction

Figure 2: Showing a stroke cycle

Chapters 2 and 3 discuss several studies showing the primarily used body parts during rowing. So, this study focuses on the kinematics involved in the various joint angles like the elbow, shoulder and pelvic joint.

Chapter 2 provides detailed information regarding the different phases of rowing and the essential joint angles to generate force for acceleration whilst rowing.

Chapter 3 provides a literature review of the previous studies in understanding the kinematics involved in rowing or para-rowing.

Chapter 4 gives detailed knowledge about the process of developing the device.

Chapter 5 tells the method to use this newly developed, markerless motion capture device.

Chapter 6 discusses the result obtained from the markerless motion capture device compared to the data obtained from the VICON motion capture system.

Chapter 7 talks through what can be done next in this study.

Chapter 8 Summarises the entire study and the main findings of this study.

Chapter 2: Background Information

Para-rowing is a competitive and recreational sport growing in popularity worldwide (Cutler, Eger et al.). Rowing is an activity that involves the function of the leg, trunk, shoulder, elbows

and wrist. Researcher Kleshnev conducted a study that showed that the legs generate 45.2±4.9% of the total propulsive force, 32.2±5.8% by the trunk, and 22.6±5.8% by the arms. This study was conducted using 88 elite rowers and found (Valery, 2003). Since this study has used an LTA set-up, so the joint angle of interest are shoulder, elbows, wrist and trunk. A study was conducted to see the effect of injuries from various risk factors, including fitness issues and improper techniques, has a significant effect on rowing (Arumugam, Ayyadurai et al. (2020)). So, the participant was asked to maintain their regular training regime. The Paralympics has allowed rowers with such disabilities to lead their lives as healthy as possible despite these obstructions.

2.1 Para-athlete Rowing Categories

The International Paralympic Committee classified the para-athlete rowing competition into three categories. These classifications are PR1 (SA - Shoulders and Arms), PR2 (TA - Trunk and Arms), and PR3 (LTA - Legs, Trunk, and Arms). The PR1 class of para-rowing is for the para-athletes with Ataxia, Athetosis, or Hypertonia from Cerebral Palsy brain injury or stroke or even people with loss of muscle strength. The PR2 class of para-rowing is for the paraathletes with no functional leg movement, due to which they are unable to slide the seat in the boat. Finally, the third type of rowing competition is the PR3, where the para-athlete has a visual or physical impairment. This impairment includes limb loss or deficiency or loss of muscle strength equivalent to spinal cord injury at S1 or minimum ataxia, athetosis, or hypertonia from Cerebral Palsy (CP) brain injury or stroke (Anon., 2021).

2.2 Phases of Rowing

There are four distinct phases in rowing — the catch, drive, finish, and recovery phase. These phases of rowing stroke are performed primarily in the longitudinal plane (Paul Thompson). The four stages of rowing are shown in Figure 3.

Figure removed due to copyright restriction

Figure 3: Different phases of rowing

The catch phase

The initial propulsion of the boat occurs in this phase by putting the rowing oar into the water and initiating the propulsion of the boat forward (Figure 3A) (Thompson & Wolf, 2016). A study conducted by Strahan and his partners showed that there is an asymmetrical movement at the catch phase due to only one oar used in sweep rowing. This asymmetrical movement is associated with rotation and lateral bending of the spine, primarily in the upper thoracic region (Strahan , et al., 2011); this is shown in Figure 4A. Maximal flexion occurs at the ankles, knees, and hip in the catch position to optimise rowing stroke length (SL) (i.e., the distance travelled by the oar travels through the water) (Mazzone, 1988).

The drive phase

The drive phase is also known as "the leg drive" and is divided into the early and late drive phases (Thompson & Wolf, 2016). The early and late drive phase is shown in Figures 4B and 5B. It has been seen in many studies that, during the early drive phase, electromyographic (EMG) activity indicates that the knee and the upper thigh region play a vital role in boat propulsion by contracting the various muscle around the knee and the upper thigh region (Fleming, et al., 2014) (Janshen, et al., 2009) (Soper & Hume , 2004) (Turpin , et al., 2011). Thus, it can be said that the legs play an essential role in rowing, but, depending on their impairment, para-athlete rowers may have little or no control over their legs. So knowing the kinematics of para-athlete rowers will help to understand how they alter the motion of the traditional stroke to compensate. Also, studies have shown that in the late drive phase, the hip and back extensor muscles also contribute to the boat's propulsion (Pollock, et al., 2009). The propulsion in the late drive phase is caused by contraction of the hip and back extensor muscles, which initiates "the body swing" (Fleming, et al., 2014) (Janshen, et al., 2009) (Soper & Hume,

2004) (Turpin , et al., 2011) (Thompson & Wolf, 2016). Several studies of the rowing stroke in sweep rowers have shown that the EMG activity of the knee, hip, and back extensors is asymmetrical during the drive phase (Buckeridge, et al., 2014) (Janshen, et al., 2009) (Parkin , et al., 2001).

Figure 4: Phases of the sculling stroke. (A) The catch phase. (B) The drive phase. (C) The finish phase (Nugent, Flanagan et al.)

The finish phase

In this phase, the legs and trunk are fully extended, and the rowing oar handles are pulled toward the subject's body, thus removing the oar from the water (Thompson & Wolf, 2016). The final phase is shown in Figures 4C and 5C. This phase is known as "the arm pull," also, several studies conducted on EMG showed that the leg muscles are not functional during this phase; instead, the majority of muscle activity is found around the shoulders and arms (Pollock, et al., 2009) (Turpin , et al., 2011). Additionally, the muscles around the trunk contribute to the layback of the stroke by decelerating trunk extension during the finish phase (Pollock, et al., 2009) (Turpin , et al., 2011).

The recovery phase

After the finish phase, the rower extends their arms away from the body, starting the recovery phase. This phase is the opposite of the drive phase (Thompson & Wolf, 2016). Therefore, in

the finish phase, the hip and knee flexion as the rower moves toward the stern of the boat, preparing for the catch phase of the next cycle (Thompson & Wolf, 2016). Previous studies have shown that, during the recovery phase, EMG activity is low around most of the muscle groups. However, the trunk and the leg muscles have shown activity (Pollock, et al., 2009), and also in some studies, the muscles around the leg and shoulder have shown activity in this phase (Fleming, et al., 2014) (Janshen, et al., 2009) (Soper & Hume, 2004). A study Valery Kleshnev (Valery, 2003) has shown that a rowing boat moves at its highest velocity during the recovery phase. So, the athlete has to balance the boat in order to stop either of the oars from touching the water surface, which would result in the reduction of the boat velocity by increasing the drag (Baudouin, et al., 2002) (Soper & Hume, 2004) (Nugent, et al., 2020).

Figure 5: Phases of the sweep rowing stroke. (A) The catch phase. (B) The drive phase. (C) The finish phase (Nugent, Flanagan et al.).

The four phases of rowing show the extensive use of the athlete's leg, trunk, and arms, but depending on the classification of the para-athlete, they cannot use all their body parts. Thus, it is necessary to understand how a para-athlete compensates to ensure that the boat remains balanced. Studying and analysing the kinematics involved in para-athletic rowing will allow us to understand the coping mechanism employed by para-athletes.

The kinematics data involved in a rowing activity will be collected using two motion capture systems to compare and validate the data acquired from the OpenPose system, software

developed by A./Prof. Domenic Thewlis against the VICON data. This study's kinematics data of interest are the hip, shoulder, elbow, and wrist joints. The motion capture system processes the video and obtains these kinematics data. So, when the processed video of a rowing activity is seen on the motion capture software display, the objects are converted to stick figures in the video by the software. The kinematics data important for this study are the various joint angles like the elbow, shoulder and pelvic. This data can be obtained from the motion capture system.

In addition, the body position of the para-athlete is also an essential factor that can be added in this study by accumulating data from the pressure matt. The body position will allow us to understand how a para-athlete copes with aiding with the obstacles like the resistance provided by the wind and the water to balance the boat. So, to get that information on the body position, a pressure mat is used. The pressure mat will covertly detect a person is standing, sitting, or walking on it.

Chapter 3: Literature Review

In the boats for Paralympic rowers, there are pontoons attached to the sides of the boat to provide stability. The pontoon is mandatory for PR1 rowers but is optional for PR2 and PR3 rowers. In addition, the seat is fixed for the SA and TA, but for the LTA, the seats may or may not be fixed. Furthermore, there are different strapping arrangements for the three categories of Paralympic rowing. For PR1, straps are available for the chest and the knee, also sometimes, additional postural straps are used. In PR2, only a knee strap is used (Anon., 2021). A study has shown that specific seating and strapping configurations and strapping positions based on their requirement as per the rules of para-rowing can also influence the performance of a pararower (Severin, et al., 2021). This study was conducted with elite para-athletes and analysed the shoulders, elbows, trunk joint angles, stroke length, peak force and several other parameters.

This study aims to capture the motion of para-athlete rowers with LTA (Legs, Trunk and Arms), or TA (Trunk and Arms), or SA (Shoulders and Arms) in outdoor environmental conditions. Researchers conducted earlier studies to capture the motion of the para-athlete for performance analysis. Still, the drawback to those studies was that all those studies used ergometers in a motion capture laboratory (Nugent & et al., 2020) (Cerasola & et al., 2020) (Wan & Sawad, 2007) (Arumugam & el al., 2020). The study conducted by Butler and his group used all three kinds of set-up: the LTA, TA, and SA with abled-bodied athletes for performing their study. This study determined the shoulders, elbows, and lumber joint angles at each phase and has discussed the change in the stroke length for every set-up (Cutler, et al., 2016).

Furthermore, many factors such as water resistance and force, wind velocity and other environmental conditions are neglected in the previous research. This factor and the rowing technics play a vital role in enhancing or weakening any athlete's performance (Holt, et al., 2020). In this research, a markerless motion capture system will be used, which will allow us to conduct the study in an outdoor environment.

Additionally, studies have been conducted to investigate the influence of rowing ergometer compliance on biomechanical and physiological parameters in an ergometer (Šarabon, et al., 2019), thus, neglecting the environmental factors. Hence, this markerless motion capture

system will allow the measurement of these biomechanical and physiological parameters more accurately.

Also, studies have been earlier conducted to determine the essential parameters in assessing the performance of a rower (Kleshnev, 1998). The drawback of this study was that it neglected the crucial environmental factors, so this markerless motion capture system would help validate if those parameters conducted to influence a rower's performance are still corrected when the external environmental factors come to play.

A study conducted by Neil Fleming and his team showed the activation of various muscle groups across each phase of the rowing cycle (Fleming, et al., 2014). Since this study focuses on para-athlete rowers with LTA set-up, the kinematics data of interest in this research are the upper body joint angles like the wrists, elbows, shoulders, and hips angle. Also, Pollok and his team conducted to study on the EMG and trunk (pelvic and spine) during rowing in elite female rowers during a complete rowing stroke. This study analysed the variation in trunk movement at the peak force (POLLOCK, et al., 2009). Therefore, from this study, the trunk muscle of the spinal segments, L3–S1, plays an important role in the propulsion of the boat. Hence it can be said that one of the essential joints is the hip joint during rowing.

Para-rowers cannot use all body parts required for rowing due to temporary or permanent injuries (Arumugam & el al., 2020). It is not yet known how para-rowers compensate for variable weather conditions in an outdoor environment. This device will be helpful for the paraathlete's coaches to determine the areas of improvement for the para-athlete. In turn, this device will help the para-athlete rowers improve their performance based on the analysis from their coach.

Earlier studies have been conducted comparing the markerless motion capture system OpenPose against a gold standard marker-based device stereophotogrammetric video system. This study aimed to analyse the accuracy of the markerless motion capture system compared to the standardised marker-based system by asking the subjects to perform a repeated activity. The result of this study confirms that by using two low-cost webcams and the OpenPose engine, it is feasible to track the kinematics and gait parameters of a single subject in a 3D space (Zago, et al., 2020). But this study was conducted indoors with random activity repeatedly, and this researcher aims to take this system on water using only one webcam. Also, this study focuses

explicitly on rowing to help deliver a markerless motion capture system that can be used in outdoor environmental conditions.

The markerless motion capture system used in this study was developed by Dr Dominic Thewlis, University of Adelaide. This system is called OpenPose. Studies have been conducted with the OpenPose system to study the kinematics in a repetitive activate. This study showed that changing the position of the camera results in the change in error (Zago, et al., 2020). This software will help monitor the different kinematics of the athlete in the natural environment. This acquired data will provide information for performance enhancement.

Chapter 4: Device Development Process

For developing this device, a few important factors had to be considered. As mentioned in the introduction, there are a few criteria whilst developing these markerless motion capture devices. This includes the device needing to be small so as to mount onto a rowing boat. Also, it needs to be portable, so the device needs to be small and lightweight. Additionally, as the completed device will be taken into the rowing environment on the water, it has to be waterresistant.

4.1 A./Prof. Dominic Thewlis's Markerless motion capture system

The markerless motion capture system developed by Dr Dominic and his group at the University of Adelaide uses the ZED2i camera, which is lightweight, portable and waterresistant. So the camera not only satisfies all requirements for a markerless motion capture system but also has features, up to 60 frames per second video capture and a focal length of 1.8m. This focal length satisfies another requirement as the length of seating is in the boat is around 2 meters from the start of the boat or ergometer, shown in Figure 6. So, the camera can capture the entire frame of the participant without any issue.

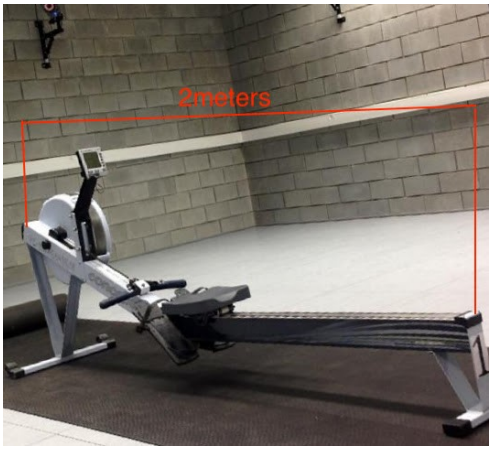

Figure 6: Length of the boat from start to the seating area

Furthermore, this markerless motion capture camera runs on the NVIDIA platform, so the Jetson Nano 2 Gb developer kit was chosen as the processor. Several issues were faced while setting up the processor, but all were successfully overcome. Firstly, the internet was required to install the ZED software package, so a Wi-fi adaptor was set-up. Since Jetson Nano is a standalone processor and not a PC, the problem was encountered. This issue was tackled by changing a few lines in the code of the 'MakeFile' of the installation software of the Wi-fi

adaptor. The changes made to the 'MakeFile' is shown in Figure 7. The solution was found on the EDiMAX Pro website (Desk, 2021). This Wi-fi adaptor is set up for the jetson nano, which will help make the device portable. This will be useful once a mobile user interface (UI) is developed, which would be the next step for this study.

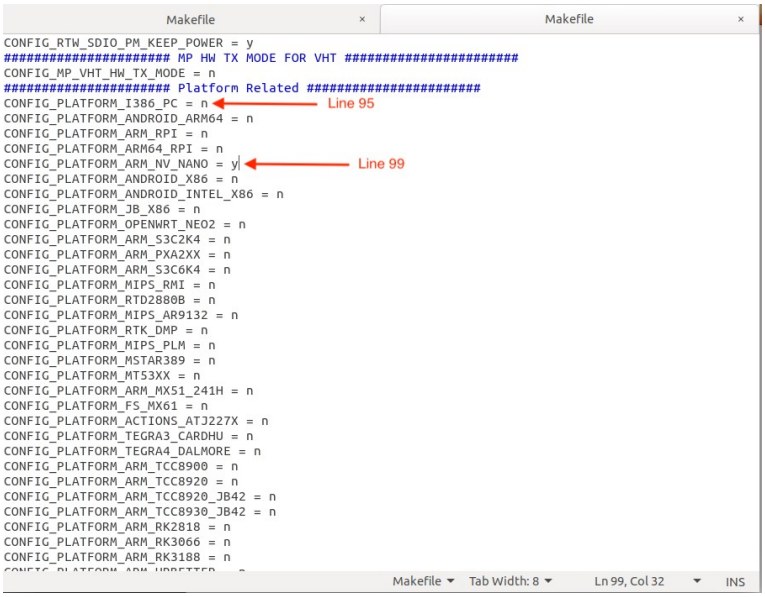

(a)

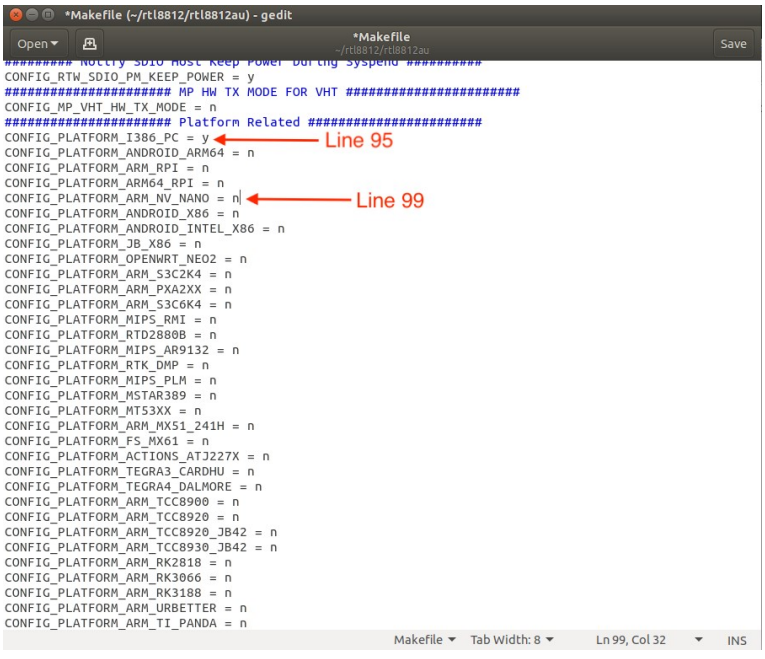

(b)

Figure 7: Changes in 'MakeFile' Code (a) Before change (b) After change

Once the markerless motion capture device was developed, data were collected simultaneously with the standardised VICON motion capture system used for kinematics analysis which is

accepted worldwide. In order to validate the developed markerless motion capture system against the standard VICON motion capture system. This validation is done in order to confirm that the developed markerless system can be used as a standalone device in an outdoor environment. Then the data for the VICON system was collected using Nexus 2.12.1, and the data from the newly developed markerless motion capture system was gathered using the software developed by A./Prof. Dominic Thewlis, University of Adelaide. This software is called OpenPose. The data obtained from the newly developed markerless motion capture system was validated against the data acquired from the VICON system.

4.1.1 OpenPose – Software developed by Dr Dominic Thewlis

The Open Pose is the software that A./Prof. Dominic Thewlis develops. This software runs a function called "05_keypoints_from_images_multi_gpu.py" from GitHub (Thewlis, 2020). The video obtained from the ZED2i camera is fed to this function, which then processes the video to give the markers' position at various joint angles (Zago, et al., 2020). The postprocessing of the ZED2i video has been done by Mr. Christopher Kurrin Whalley, a Master student of A./Prof. Dominic. The marker set of the OpenPose is different from that of the VICON system shown in Appendix 1.C. The marker set for the OpenPose software is shown in Figure 8, and Table 1 shows what the numbering represents.

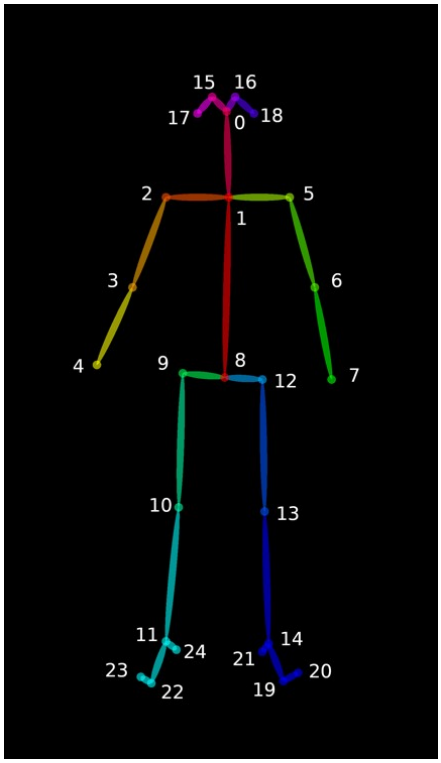

Figure 8: Marker set for the OpenPose System

From Figure 8, it can be seen that the OpenPose system doesn't have a marker set for the fingers; thus, it is not possible to obtain the data for the wrist angle. Therefore, the joints to consider for data analysis are the elbow, shoulder, and hip joint (LTA set-up).

Table 1: Representation of the marker set for the OpenPose system

Marker Number	Marker Placement	Marker Number	Marker Placement
0	Nose	12	Left Hip
1	Neck	13	Left Knee
2	Right Shoulder	14	Left Ankle
3	Right Elbow	15	Right Eye
4	Right Wrist	16	Left Eye
5	Left Shoulder	17	Right Ear
6	Left Elbow	18	Left Ear
7	Left Wrist	19	Left Big Toe
8	Mid Hip	20	Left Small Toe
9	Right Hip	21	Left Heel
10	Right Knee	22	Right Big Toe
11	Right Ankle	23	Right Small Toe
		24	Right Heel

Chapter 5: Methodology

In this study, an abled-body rower was asked to perform certain rowing activities on a Concept2 Model D with fixed seats and an indoor rowing ergometer used for all trials. The participants had to sign a consent form before starting the study, which has been approved by the South Australia (SA) Health Human Research Ethics Committee (HREC). The project ID number approved by the SA HREC is 4345. The participant was an able-bodied athlete familiar with the Concept2 Model D ergometer but had no previous experience with para-rowing LTA set-ups.

5.1 Marker placement

The motion capture tool kit module of the computer simulation software VICON Nexus 2.12.1 requires specific placements of the 39 spherical marker sets. The participant's upper and lower body was marked with the spherical marker sets, as shown in figure 9(a) and appendix 1.A and 1.B and the names for all the marker placements are shown in Appendix 1.C, considering the LTA ergometer set-up. For this study, the 14mm traditional spherical base markers were stuck to the participant's skin or cloth with a double-sided adhesive material. Then the VICON camera system was calibrated and set its origin in the Rehab & Motion Analysis Laboratory, Flinders University. After configuring the VICON camera system, the participant was asked to stand in a T-pose, as shown in figure 9(b). This is required for storing the participant's body dimensions, also a requirement for the VICON software.

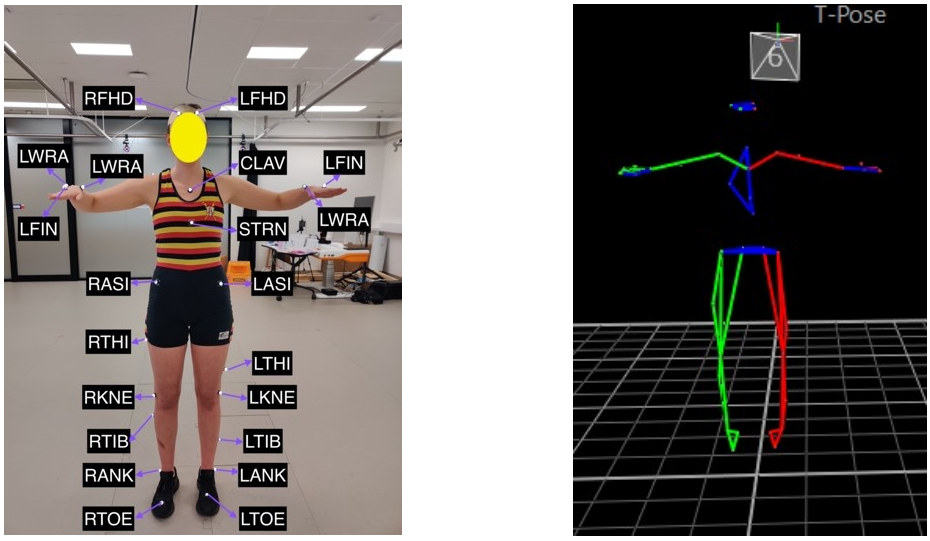

(a) (b)

Figure 9: (a) Stick figure of the T-Pose (b) T-pose along with the marker set used

5.2 Experimental set-up for VICON System

For data collection, calibrating the VICON camera system was done in the Rehab & Motion Analysis Laboratory, Flinders University. Firstly, open the Nexus 2.11 and turn on the Go Live mode and click on the 'Start' button under the 'Camera Calibration' section in the 'Tools' area on the right side of the software window, shown in Figure 10. Next, start waving the T- wand while walking around the centre of the laboratory where the ergometer will be set up. Keep the 'image Error' less than 0.1 for the best result; else, 0.15 is ok but not the best. The result of the calibration of the ten cameras of the VICON system is shown in Figure 11. Finally, set the origin of the room. The final camera set-up for the VICON system is shown in Figure 12.

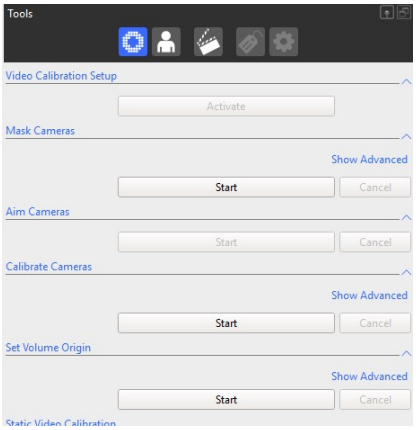

Figure 10: Toolbox for VICON camera system calibration and set its origin

Camera	Wand Count	World Error	Image Error
#1 (Bonita 10)	1838	0.148473	0.0979993
#2 (Bonita 10)	2187	0.2484	0.141621
#3 (Bonita 10)	2150	0.338635	0.0992689
#4 (Bonita 10)	1916	0.344139	0.104005
#5 (Bonita 10)	1001	0.335628	0.107902
#6 (Vero v2.2)	2505	0.182587	0.0836119
#7 (Bonita 10)	2669	0.201301	0.060838
#8 (Bonita	2180	0.320383	0.110442

Figure 11: Calibration result for the VICON system

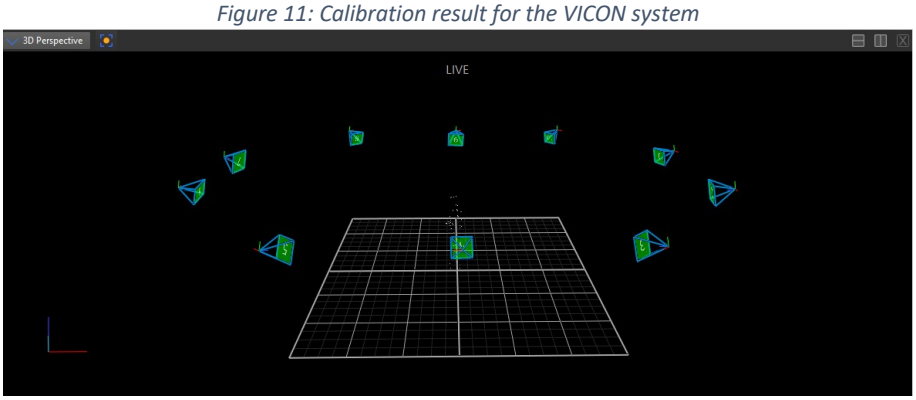

Figure 12: 3D camera view for the VICON system

5.3 Experimental set-up for ZED2i Camera System

The ZED2i camera system was set up by calibrating the camera system. Calibration of the system was done by opening the "calibrating ZED" software in the directory "cd

usr/local/ZED/tools" of the Jetson Nano 2GB Development kit processor. Then click on the "Start" button on the PC's screen, depicted in Figure 13.

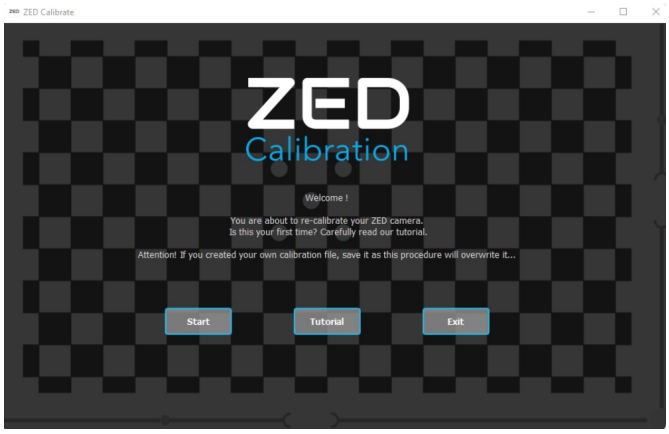

Figure 13: How to start calibrating the ZED2i camera system

During the calibration process, the target is to project the blue dot on top of the red dot, such that both are of identical shape and size, as shown in Figure 14. To adjust the size of the blue dot, the ZED2i camera is moved forwards or backwards. To change the shape of the blue dot, the camera system is adjusted laterally or longitudinally at an angle. Also, the dot on the right and the bottom of the screen should be within the bracket ( ). Now to get the dot on the right sideline within the bracket, the camera is moved longitudinally and to get the dot on the bottom line within the bracket by adjusting the camera system laterally. Once all these conditions are satisfied, the spot turns green, roughly around 5 seconds later. This process will be repeated several times.

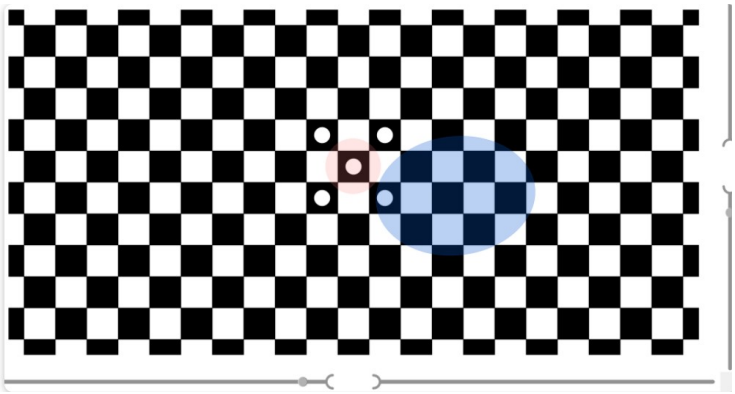

Figure 14: Calibrating process

5.4 Pilot Testing

Pilot testing was conducted to determine the optimal camera (ZED2i) position of the markerless motion capture system that should be used for testing. The pilot testing was conducted to capture the participant performing the rowing activity in the frame without missing any major joint angles. So that the system does not miss out on capturing any data of interest, it is essential to check if the system is capturing all the significant joint angles.

The trial of pilot testing was done only using the kinematic aspect of the analysis. The reason for this was to obtain all major joint angles. This helped in determining the position and angle at which the camera was positioned. So, the final set-up for the markerless motion capture camera (ZED2i) is shown in Figure 15. It was set up on top of a tripod in front of the Concept2 ergometer. The camera lens of the ZED2i was set up at an angle of 23° keeping the horizontal black rod on the tripod as the base. The height of the tripod was adjusted to the height of the participant.

(a)

(b)

Figure 15: ZED2i camera set-up for markerless motion capture system (a) Frontal view (b) Lateral view

5.5 Trial Process

The participant was then asked to warm up for 5 minutes. After which, the participant was asked to complete 12-strokes trials for each stroke rate. The stroke rate chosen was 24spm (stroke rate per minute), 28spm, 32spm, and 40spm. This set of stroke rates was decided after discussing with the para-athlete rowing coaches of the South Australian Sports Institute (SASI). Data was collected by synchronising both the camera systems, that is, the camera system for the VICON and the ZED2i camera system. For synchronising, the participant was asked to raise their arms before staring at the data recording in both approaches.

Chapter 6: Data Processing

6.1 Post-processing of VICON data

After recording the video, the data was collected using NEXUS 2.12.1 for the VICON system. For compiling the data, firstly, each of the trails the recording was pipelined using the icon circled in Figure 16. Secondly, analysis was done for each of the videos, frame by frame, and if any of the markers were missing, then manually added those markers. Finally, the joint angle data was collected for the wrists, elbows, shoulders, hips, pelvis, neck, and thorax angle in .csv format.

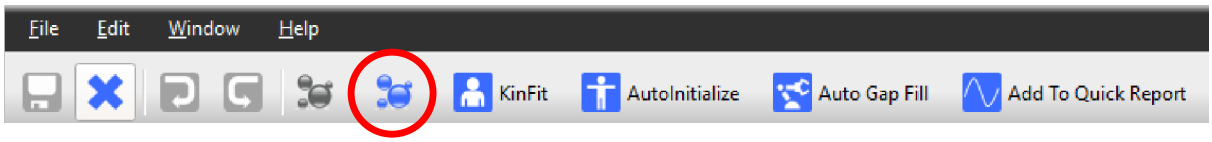

Figure 16: Pipeline icon

6.2 Post-processing of OpenPose system

The newly developed markerless motion capture system data was gathered using the software developed by A./Prof. Dominic, OpenPose. With the help of Mr Christopher Kurrin Whalley, data was accumulated from the recording acquired from the ZED2i camera. This was done by processing the video in OpenPose by running the function "05_keypoints_from_images_multi_gpu.py" from GitHub (Thewlis, 2020) and followed by noise removal for frequency over 120Hz from this data using the Butterworth filter. Finally, the data for the maker position of the wrists, elbows, shoulders, and hips joints was gathered in .csv format. Then from the collected position data of the markers, the join angles were derived by calculating the position vector followed by dot product($a.\ b = |a||b|cos\theta$) Corresponding position vectors at the joint. These acquired joint angle data is in the local coordinate system.

The data obtained from the developed markerless motion capture system was compared to the data acquired from the VICON system. Since the OpenPose system, data was collected of joint position for the wrists, elbows, shoulders, hips, and knee positions to calculate the joint angles for the wrists, elbows, shoulders, and hips angles, as LTA para-rowing set-up was used for the trial. So, each of these joint angle data for each phase of the cycle was compared to the data

collected from the standardised VICON system for each of the stroke rates. These results have been discussed in Chapter 7.

Chapter 7: Results

Figures 17, 18, 19, and 20 shows a phase of a complete rowing cycle of 24spm data set for both systems. The 'orange' line represents the data set acquired from the VICON system, and the 'blue' line denotes the data set obtained from the ZED2i system. The x-axis of this graph depicts the time in seconds (sec), and the y-axis of this graph represents the time in degrees (deg°).

The following graphs show the three complete strokes of a rowing cycle of the ZED2i markerless motion capture system and the VICON motion capture system. The elbow and the hip joint angles were taken in the 'x' coordinate, and the shoulder angle was taken in the 'y' coordinate of the 3-D coordinate system.

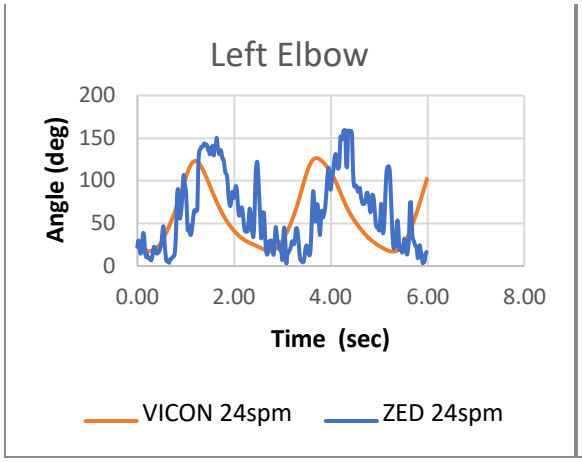

(a)

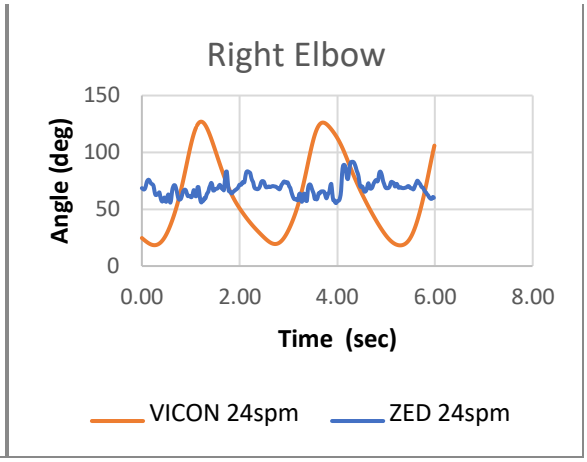

(b)

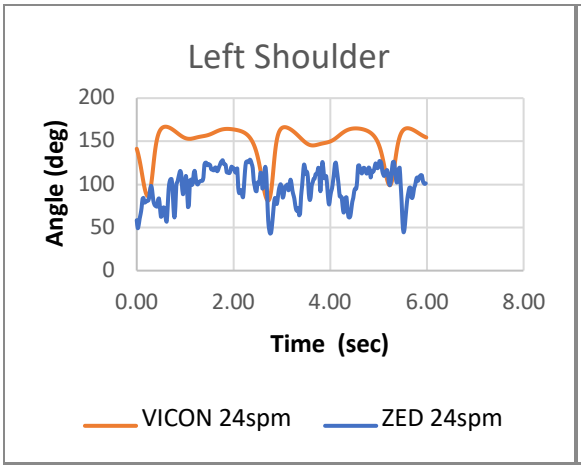

(c)

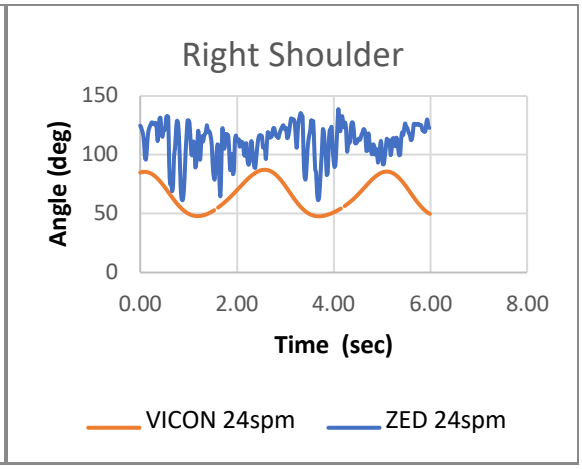

(d)

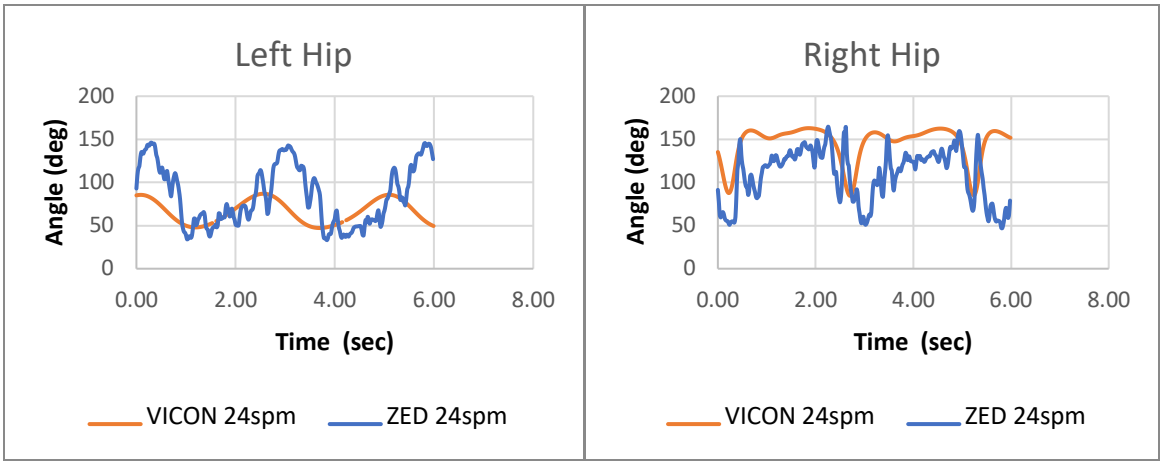

(e) *(f)*

Figure 17: Graphs validating a phase for 24spm of ZED2i against VICON data (a) and (b) Elbow, (c) and (d) Shoulder, and (e) and (f) Hip

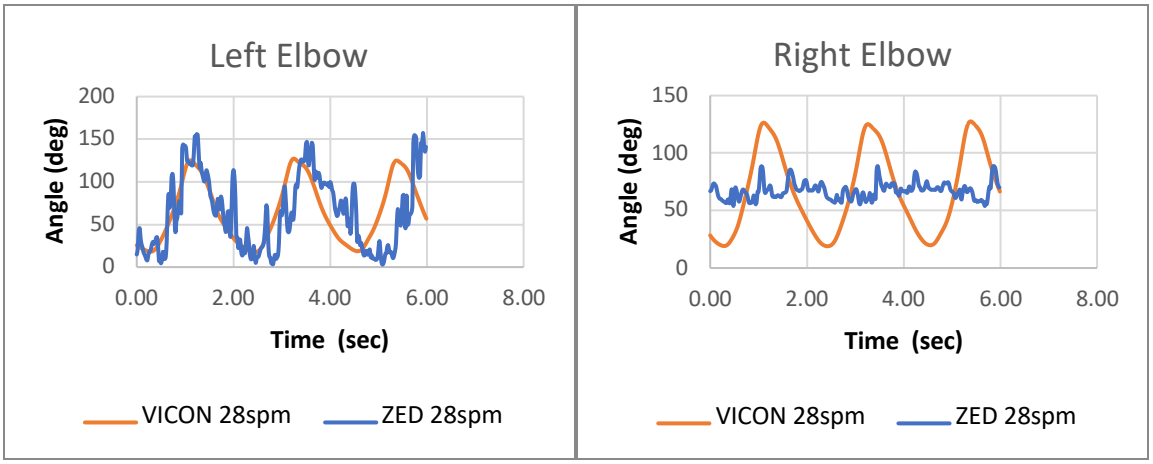

(a) *(b)*

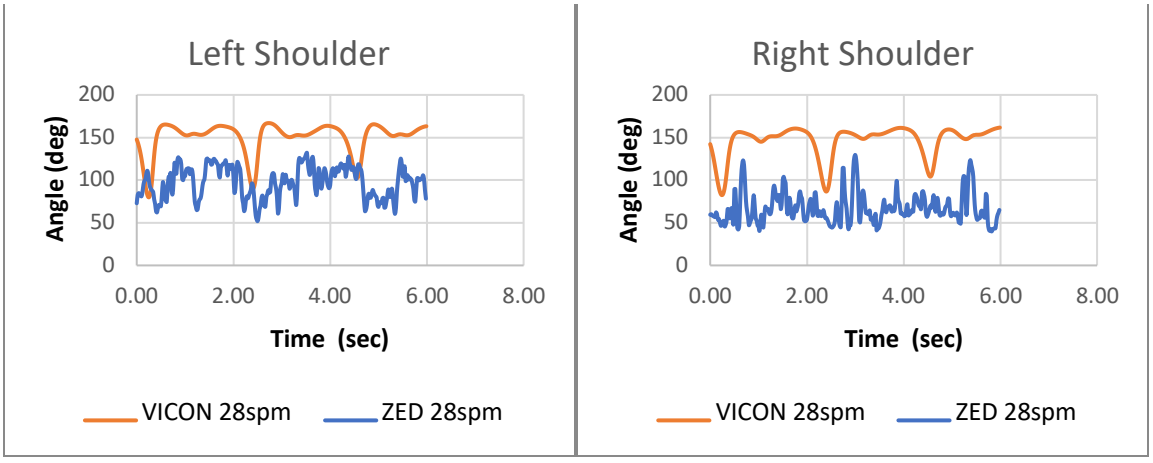

(c) *(d)*

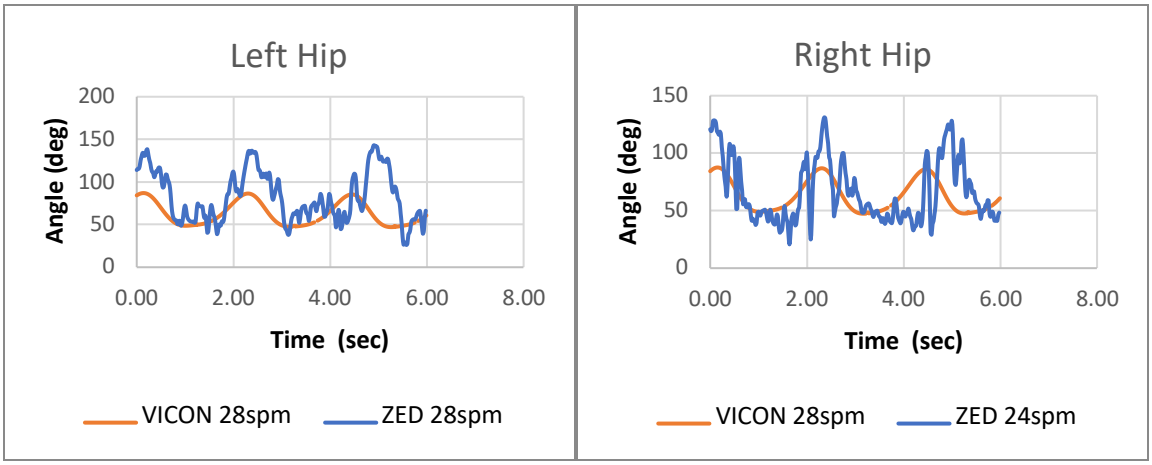

(e) *(f)*

Figure 18: Graphs validating a phase for 28spm of ZED2i against VICON data (a) and (b) Elbow, (c) and (d) Shoulder, and (e) and (f) Hip

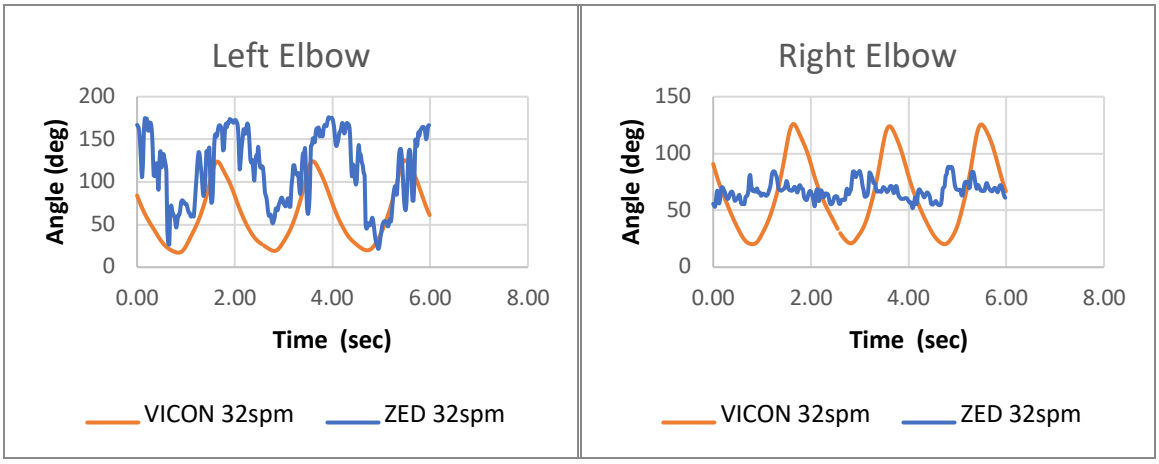

(a) *(b)*

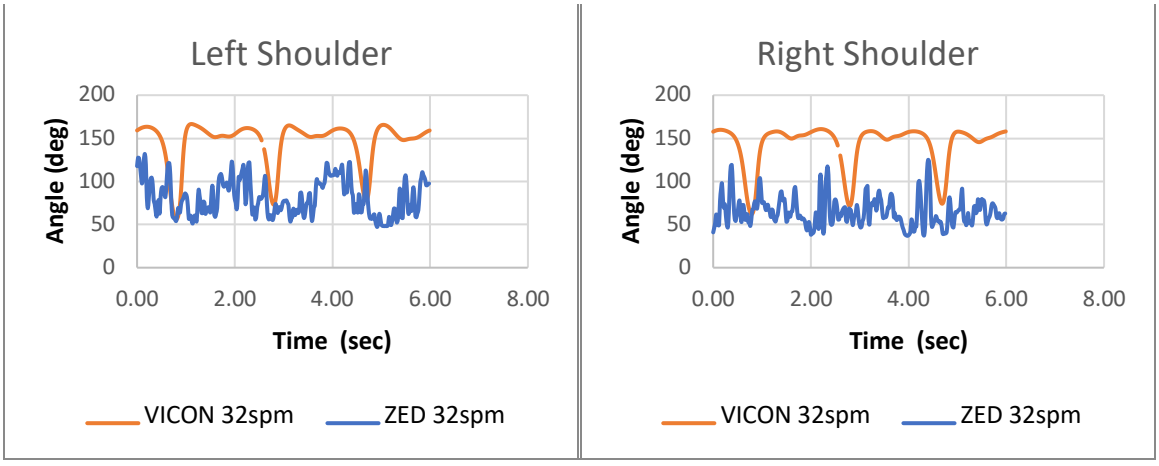

(c) *(d)*

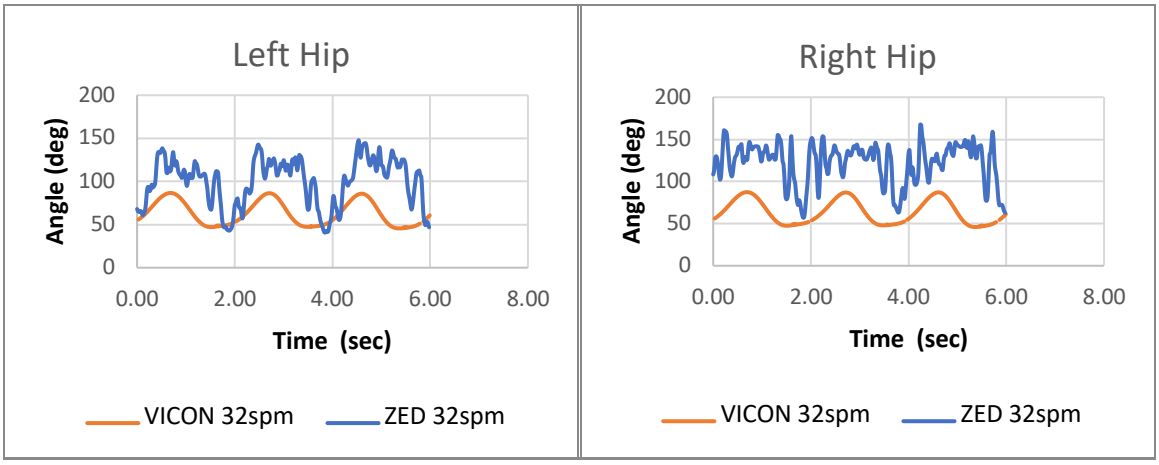

(e) *(f)*

Figure 19: Graphs validating a phase for 32spm of ZED2i against VICON data (a) and (b) Elbow, (c) and (d) Shoulder, and (e) and (f) Hip

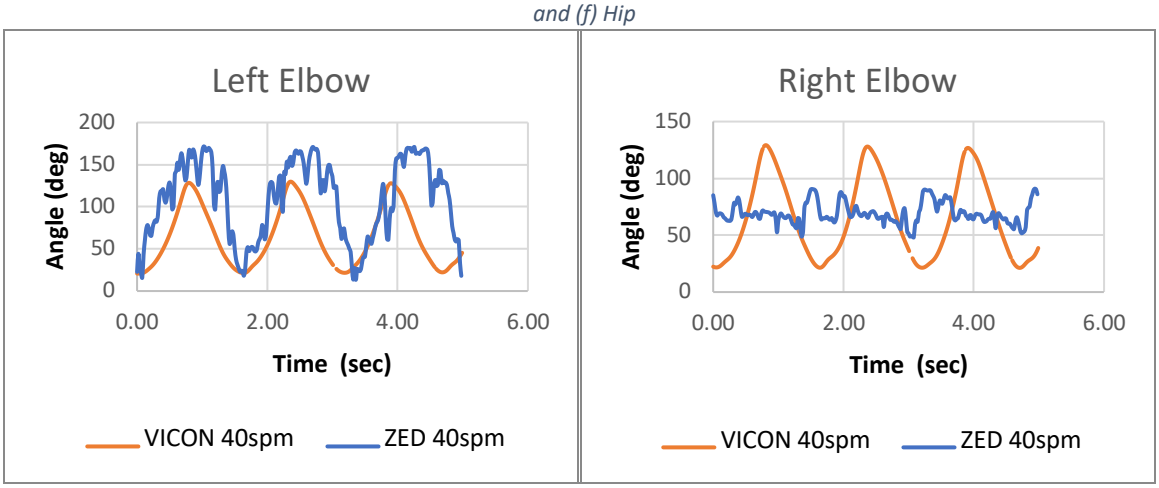

(a) *(b)*

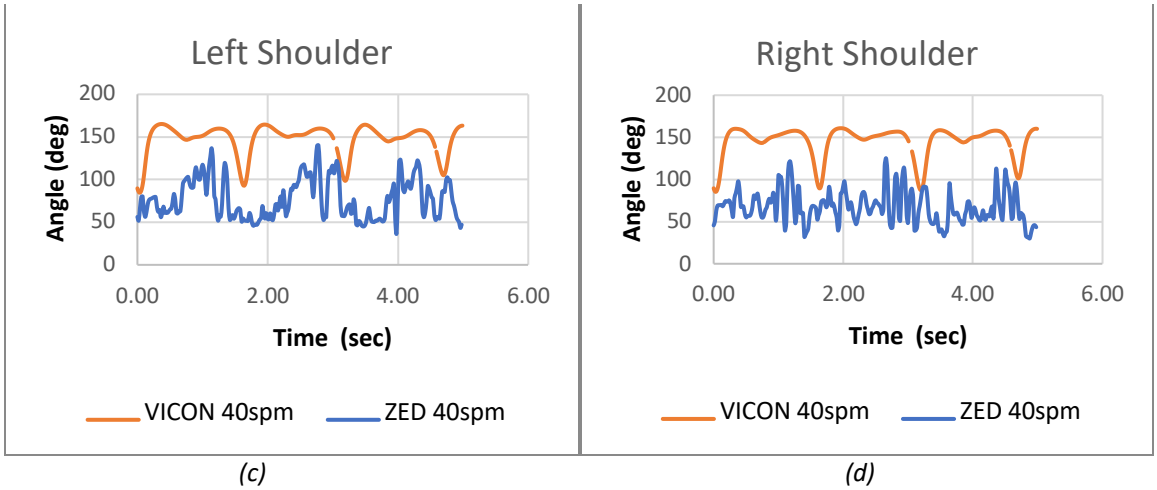

(c) *(d)*

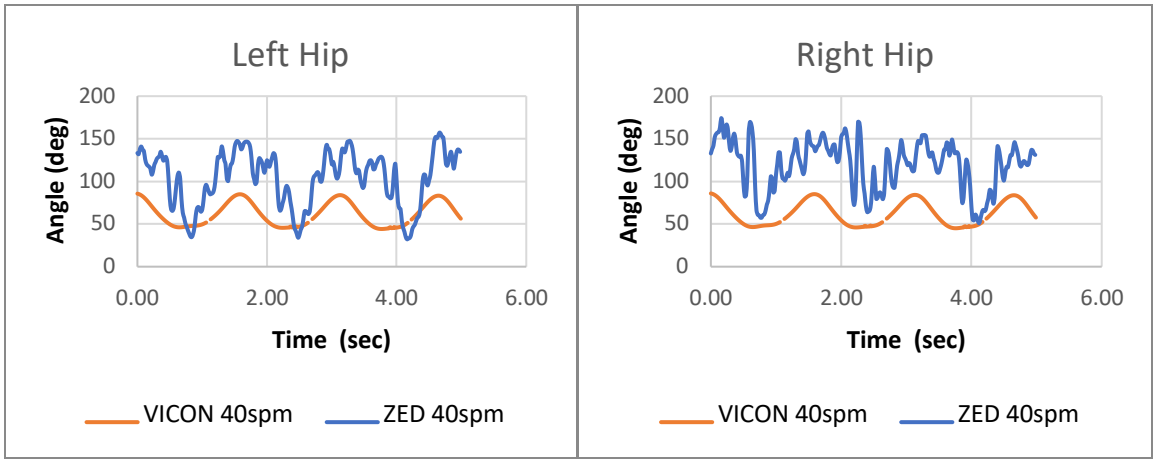

(e) *(f)*

Figure 20: Graphs validating a phase for 40spm of ZED2i against VICON data (a) and (b) Elbow, (c) and (d) Shoulder, and (e) and (f) Hip

Chapter 8: Discussions

As stated in the introduction, this research aims to study three entire strokes of a complete rowing cycle. This is done to study the change in three full rowing cycles stroke. If the change in phase for the ZED2i and the VICON system are identical, then the ZED2i system can be used to study the para-athletic rower's kinematics. The steps taken to achieve this goal and the result is discussed in this chapter.

For extracting a phase from a complete cycle, the ZED2i data was processed with 50Hz, and the VICON data was processed with 100Hz. This was done because the VICON camera system captures data at 100Hz frequency, and the ZED2i camera system captures data at 50Hz frequency for the position sensor (Inc., 2021). This process was carried out to extract a stroke cycle from the entire data set. This process was followed throughout all the stroke rate data, that is, 24spm, 28spm, 32spm and 40spm.

Next, coordinates were chosen for each of the joints. The elbow and the hip joint angles were taken in the 'x' coordinate of the 3-D coordinate system. Figures 4 and 5 show maximum change in the hip and elbow joint angles and a slight change in the shoulder joint angle during the different phases of the rowing cycle. But from the data acquired from the VICON system, it was observed that the joint angles in the y and the 'z-axis are negligible, or noise, but the 'x' coordinate showed clear recording for the elbow and the hip joint angle. For the shoulder angle 'y' coordinate of the 3-D coordinate system was taken.

Then 12 strokes for each stroke rate were extracted by removing all the data points from the start and the end, where the participant was asked to raise their hand. The data was significantly different for the period when the participant's hand was raised, so it was easy to analyse the 12 strokes of interest. When the 12 stoke cycle of the ZED2i data was overlapped with the VICON system data, it was observed that the phases of the stroke cycles were inverted to that of the VICON system. Thus, a 180° phase shift was applied to all the shoulder data across all the stroke rates.

Furthermore, three consecutive stroke cycles were selected from VICON data overlapped with the ZED2i data for the same stroke cycles for all the joint angles. This process was carried out for all the stroke rates.

From the graphs of Figure 17 (a, c, e, and f), Figure 18 (a, c, e, and f), Figure 19 (a, c, e, and f) and Figure 20 (a, c, e, and f), it can be concluded that the stroke cycles are in phase with each other for both the systems. Thus, it can be said that the x-direction of both systems is in the same direction. Additionally, it can be said that the y-direction of both the systems are opposite to each other since all the shoulder data for the ZED2i was processed with 180° to get the data in phase with the VICON data.

Also, the data obtained from the ZED2i shows a lot of variation in the joint angles. This variation in the joint angles is because the OpenPose system assumes a marker position when it can't see the joint position. From Figure 8 and Appendix 1.A and 1.B, it can be seen that the marker position of the ZED2i for all the joint positions is different from the VICON system marker set. Thus, resulting in a change of the angles.

Additionally, in all the recordings, that is, 24spm, 28spm, 32spm and 40spm, shown in Figure 17, 18, 19, and 20, it can be seen that the data for the joint angles farthest from the ZED2i camera; that is, the right elbow and the right and left shoulder data were not clear, for the ZED2i. This could be due to the camera's positioning, or else this study would require 2 ZED2i camera sets to conduct this study, as studies have shown that changing the position of the ZED2i changes the error (Zago, et al., 2020). Using two sets of camera systems will solve the issue of OpenPose predicting marker positions, especially for the joint angles far from the ZED2i camera.

Chapter 9: Conclusion

The data gathered from the ZED2i OpenPose markerless system needs to be tried out with different positioning of the ZED2i camera before it can be used as a standalone motion capture system for collecting kinematics data in an outdoor environment. So the camera position needs to be altered else, or 2 ZED2i camera sets need to be used to conduct this study to get the data from two directions.

Chapter 10: Future Study

Future work requires a complete understanding of how a para-athlete rower can tackle environmental obstacles. First, the study needs to be conducted with para-athlete rowers. For this, the drag unit [DU] for ergometer resistance needs to be set up as defined in Table 2 (Lewis, n.d.)

Table 2: Drag Unit [DU] for ergometer according to gender, weight and different category of para-athlete rowing

	LTA	TA	SA
Male Rower			
Lightweight (<160lbs or 72.57kg)	120	135	165
Heavyweight (>160lbs or 72.57kg)	130	140	175
Female rower			
All	110	125	150

Secondly, this study needs to be conducted by placing the camera in front of the ergometer. If changing the positions does not solve this issue, this study needs to be undertaken with a 2 ZED2i camera set to adequately capture all the joint angles.

Additionally, a mobile user interface (UI) needs to be developed to make the markerless motion capture device mobile. This Wi-fi network has already been set up for this system.

Furthermore, this study needs to be undertaken using OpenSim, a software developed by A./Prof. Domenic. To check which software gives a better result, OpenPose or OpenSim.

Finally, the body position of the para-athlete is also an essential factor that can be added in this study by accumulating data from the pressure matt. The body position will allow us to understand how a para-athlete copes with the obstacles like the resistance provided by the wind and the water to balance the boat. So, to get that information on the body position, a pressure mat is used. The pressure mat will covertly detect a person is standing, sitting, or walking on it.

Bibliography

Mazzone, T., 1988. Sports performance series: Kinesiology of the rowing stroke. *National Strength & Conditioning Association Journal,* p. 4–13.

Šarabon, N., Kozinc , Ž., Babič, J. & Marković, G., 2019. Effect of Rowing Ergometer Compliance on Biomechanical and Physiological Indicators during Simulated 2,000-metre Race. *Journal of Sports Science and Medicine,* pp. 264-270.

Anon., 2021. *Rowing Australia.* [Online]
Available at: https://rowingaustralia.com.au/development/para-rowing/para-rowingequipment/

Anon., 2021. *Rowing New South Wales.* [Online]
Available at: https://www.rowingnsw.asn.au/beginners/pararowing/

Arumugam, S. & el al., 2020. Rowing Injuries in Elite Athletes: A Review of Incidence with Risk Factors and the Role of Biomechanics in Its Management.. *Indian Journal of Orthopaedics.*

Baudouin, A., Seiler, S. & Hawkins, D., 2002. A biomechanical review of factors affecting rowing performance. *Br J Sports Med.,* p. 396–402.

Buckeridge, E. M., Bull, A. M. J. & McGregor , . A. H., 2014. Foot force production and asymmetries in elite rowers. *Sports Biomech.,* pp. 47-61.

Cerasola, D. & et al., 2020. Predicting the 2000-m Rowing Ergometer Performance from Anthropometric, Maximal Oxygen Uptake and 60-s Mean Power Variables in National Level Young Rowers.. *Journal of Human Kinetics,* pp. 77-83.

Cutler, B., Eger, T., Merritt, T. & Godwin, A., 2016. Comparing para-rowing set-ups on an ergometer using kinematic movement patterns of able-bodied rowers. *Journal of Sports Sciences.*

Desk, F. S., 2021. *EDiMAX Pro.* [Online]
Available at: https://edimax.freshdesk.com/support/solutions/articles/14000032146-howto-install-ew-7811-ac600-series-and-ew-7822uac-adapters-on-raspberry-pi

Fleming, N., Donne, B. & Mahony, N., 2014. A comparison of electromyography and stroke kinematics during ergometer and on-water rowing. *Journal of sports science,* p. 1127– 1138.

Fleming, N., Donne, B. & Mahony, N., 2014. A comparison of electromyography and stroke kinematics during ergometer and on-water rowing. *Journal of Sports Sciences,* 32(12), p. 1127–1138.

Holt, A. C. et al., 2020. Technical Determinants of On-Water Rowing Performance. *Frontiers in Sports and active living.*
Holt, A. C. & et al., 2020. Technical Determinants of On-Water Rowing Performance.. *Frontiers in Sports and Active..*

Inc., S., 2021. *StereoLabs.* [Online]
Available at: https://www.stereolabs.com/zed-2i/

Jürimäe, T. et al., 2010. Cortell-Tormo JM, et al. Relationship between rowing ergometer performance and physiological responses to upper and lower body exercises in rowers. *J Sci Med Sport.,* p. 434–437.

Janshen, L., Mattes, K. & Tidow , G., 2009. Muscular coordination of the lower extremities of oarsmen during ergometer rowing. *J Appl Biomech,* p. 156–164.

Kleshnev, V., 1998. Estimation of Biomechanical Parameters and Propulsive Efficiency of Rowing. *Australian Institute of Sport.*

Lewis, K., n.d. Special considerations for adaptive rowing. *Rowing faster,* Volume 2nd Edition, p. 197–207.

Nugent, F. J. & et al., 2020. Strength and Conditioning for Competitive Rowers.. *STRENGTH AND CONDITIONING JOURNAL..*

Nugent, F. J., Flanagan, E. P., Wilson, F. & Warrington, G. D., 2020. Strength and Conditioning for Competitive Rowers. *Strength and Conditioning Journal.*

Parkin , S., Nowicky, A. V., Rutherford, O. M. & McGregor, A. H., 2001. Do oarsmen have asymmetries in the strength of their back and leg muscles?. *J Sports Sci.,* p. 521– 526.

POLLOCK, C. L. et al., 2009. Electromyography and Kinematics of the Trunk during Rowing in Elite Female Rowers. *Med Sci Sports Exerc.,* pp. 628-436.

Pollock, C. L. et al., 2009. Electromyography and kinematics of the trunk during rowing in elite female rowers. *Med Sci Sports Exerc.,* p. 628–636.

Severin, A. C. et al., 2021. Case Report: Adjusting Seat and Backrest Angle Improves Performance in an Elite Paralympic Rower. *Frontiers in Sports and Active living.*

Soper , C. & Hume , P. A., 2004. Towards an ideal rowing technique for performance : the contributions from biomechanics. *Sports Med,* p. 825–848.

Soper, C. & Hume, P. A., 2004. Towards an ideal rowing technique for performance : the contributions from biomechanics. *Sports Med.,* p. 825–848.

Soper, C. & Hume, P. A., 2004. Towards an ideal rowing technique for performance : the contributions from biomechanics. *Sports Med. ,* pp. 825-848..

Strahan , A. D. et al., 2011. Differences in spinopelvic kinematics in sweep and scull ergometer rowing.. *Clinical Joulnal of Sports Medicine,* p. 330–336.
Thewlis, D., 2020. *GitHub.* [Online]
Available at: https://github.com/CMU-Perceptual-Computing-Lab/openpose/tree/master/examples/tutorial_api_python

Thompson, P. & Wolf, A., 2016. Training and technique.. In: *Training for the Complete Rower..* United Kingdom: The Crowood Press Ltd, pp. 19-37.

Turpin , N. A., Guével, A., Durand, S. & Hug, F., 2011. Effect of power output on muscle coordination during rowing. *Eur J Appl Physol.,* p. 3017–3029.

Valery, K., 2003. *Rowing Biomechanics Newsletter.,* Bruce, Australia: Australian Insitute of Sport.

Wan, K. & Sawad, H., 2007. 3D Motion prediction of human upper body by tracking reflective markers on a moving body.

Zago, M., Luzzago, M. & Marangoni, T., 2020. 3D Tracking of Human Motion Using Visual Skeletonization and Stereoscopic Vision. *frointiers in bioengineering and biotechnotogy .*

Zago, M. et al., 2020. 3D Tracking of Human Motion Using Visual Skeletonization and Stereoscopic Vision. *Frontiers in Bioengineering and Biotechnology.*

Appendix

Appendix 1: Upper and Lower body Markers placements.

A. Upper body marker placement.

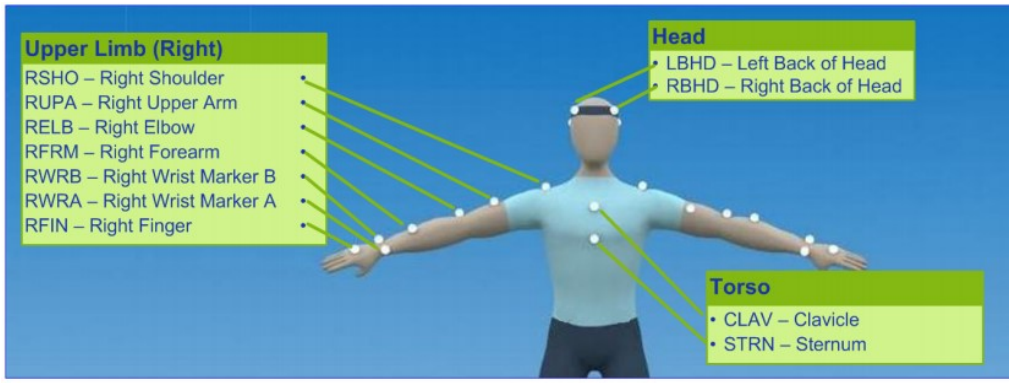

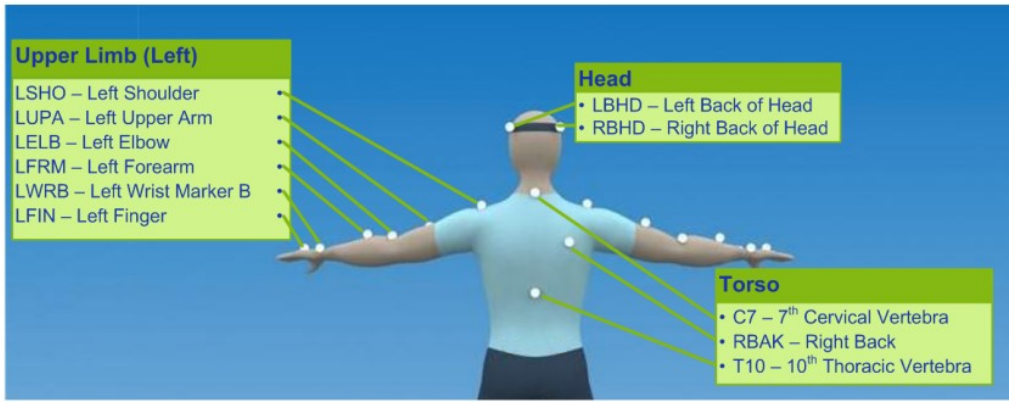

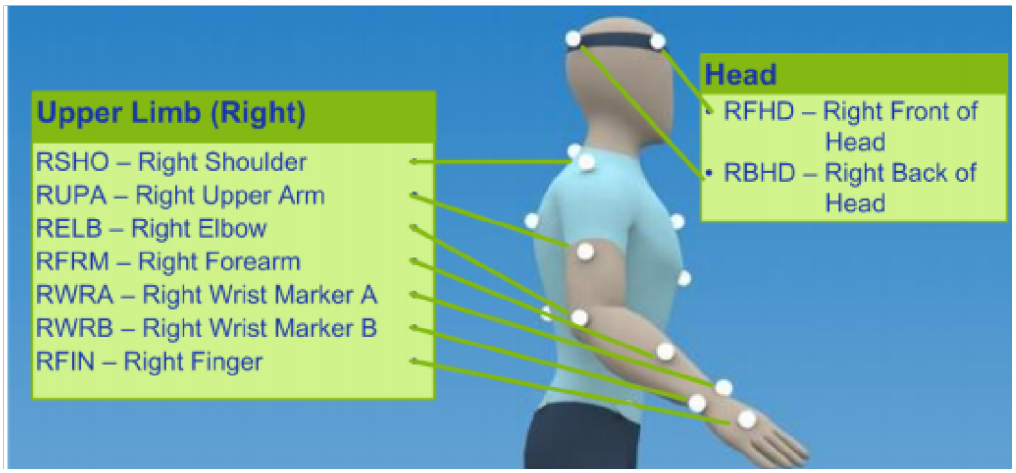

B. Lower body marker placement

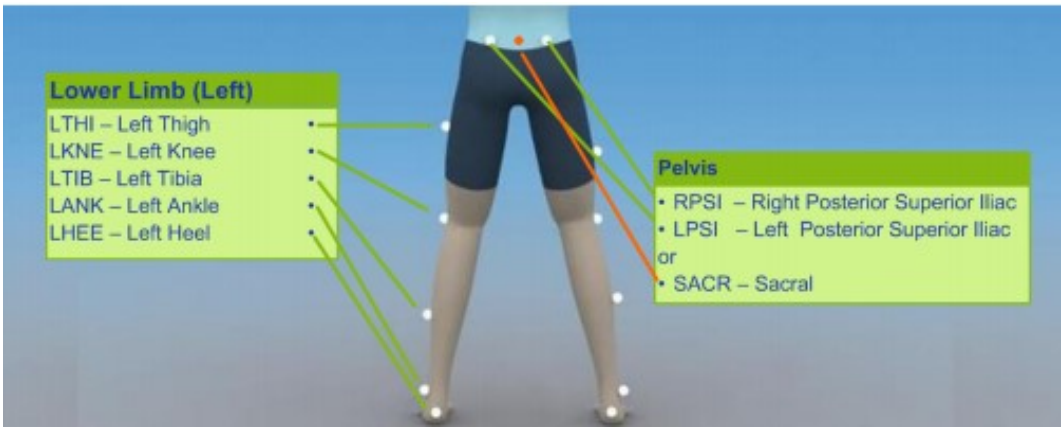

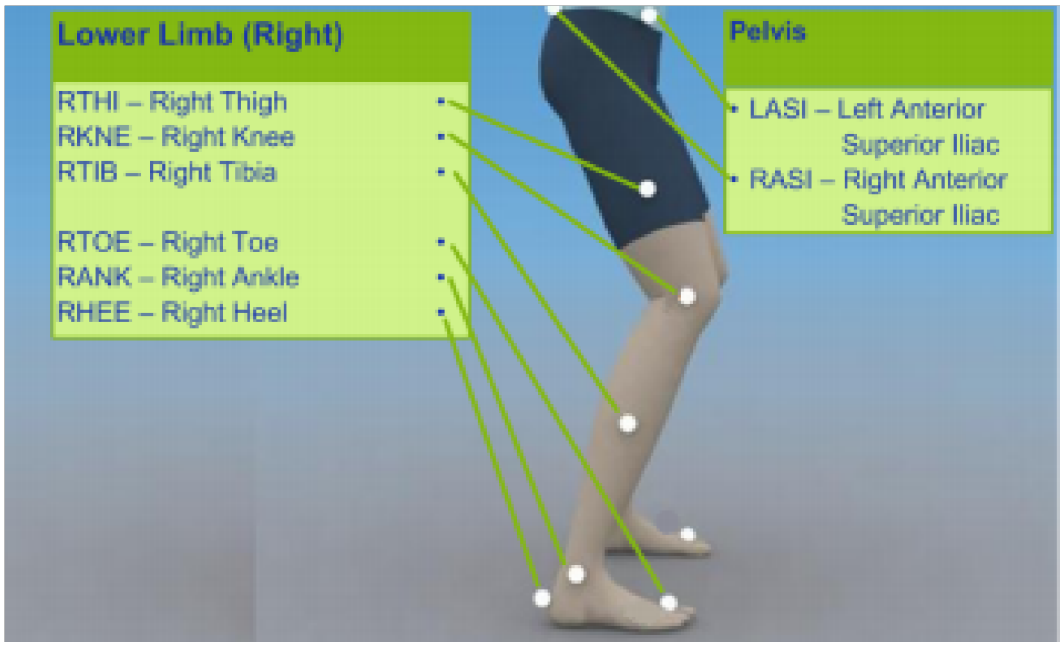

C. Placement of the Markers

Marker	Location	Description
LFHD	Left Front Head	Left Temple
RFHD	Right Front Head	Right Temple
LBHD	Left Back Head	Left-back of the head
RBHD	Right Back Head	Right-back of head
C7	7th Cervical Vertebrae	On the spinous process of the 7th cervical vertebra
T10	10th Thoracic Vertebrae	On the spinous process of the 10th thoracic vertebra
CLAV	Clavicle	On the jugular botch where the clavicle meets the sternum
STRN	Sternum	On the xiphoid process of the sternum
RBAK	Right-back	Anywhere over the right scapula
LSHO	Left Shoulder	On the acromioclavicular joint

LUPA	Left Upper Arm	On the upper lateral 1/3 surface of the left arm

LELB	Left Elbow	On the lateral epicondyle
LRRA	Left Wrist Marker A	At the thumb side of the wrist on the posterior of the left wrist, as close to the wrist joint centre as possible.
LWRB	Left Wrist Marker B	At the little finger side of the wrist on the posterior of the left wrist, as close to the wrist joint centre as possible
LFIN	Left Finger	Just proximal to the middle knuckle on the left hand
RSHO	Right Shoulder	On the acromioclavicular joint
RUPA	Right Upper Arm	On the lower lateral 1/3 surface of the right arm
RELB	Right Elbow	On the lateral epicondyle approximating the elbow joint axis
RFRM	Right Forearm	On the lower lateral 1/3 surface of the right forearm
RRRA	Right Wrist Marker A	At the thumb side of the wrist on the posterior of the left wrist, as close to the wrist joint centre as possible.
RWRB	Right Wrist Marker B	At the little finger side of the wrist on the posterior of the left wrist, as close to the wrist joint centre as possible
RFIN	Right Finger	Just below the middle knuckle on the right hand
LASI	Left ASIS	Left anterior superior iliac spine
RASI	Right ASIS	Right anterior superior iliac spine
LPSI	Left PSIS	Left posterior superior iliac spine (at the point where the spine joins the pelvis)
RPSI	Right PSIS	Right posterior superior iliac spine (at the point where the spine joins the pelvis)
LTHI	Left Thigh	Over the lower lateral 1/3 surface of the left thigh. On the line made by the left hip joint and knee marker.
LKNE	Left Knee	On the flexion-extension axis of the left knee
LTIB	Left Tibia	Over the lower 1/3 surface of the left shank. On the line made by the left knee and ankle marker.
LANK	Left Ankle	On the lateral malleolus along an imaginary line that passes through the transmalleolar axis
LHEE	Left Heel	On the calcaneous at the same height above the plantar surface of the foot as the toe marker
LTOE	Left Toe	Over the second metatarsal head, on the mid-foot side of the equinus break between fore-foot and mid-foot

RTHI	Right Thigh	Over the upper lateral 1/3 surface of the right thigh. On the line made by the right hip joint and knee marker.
RKNE	Right Knee	On the flexion-extension axis of the right knee
RTIB	Right Tibia	Over the upper 1/3 surface of the right shank. On the line made by the right knee and ankle marker.
RANK	Right Ankle	On the lateral malleolus along an imaginary line that passes through the transmalleolar axis
RHEE	Right Heel	On the calcaneous at the same height above the plantar surface of the foot as the toe marker
RTOE	Right Toe	Over the second metatarsal head, on the mid-foot side of the equinus break between fore-foot and mid-foot